Beyond Metrics and Morphology: the potential of FTIR-ATR and chemometrics to estimate age-at-death in human bone

Mariana Pedrosa[1,2,3*]; Francisco Curate[1,2,4,5]; Luís A. E. Batista de Carvalho[3]; Maria Paula M. Marques[2,3]; Maria Teresa Ferreira[1,4]

[1]Laboratory of Forensic Anthropology, Centre for Functional Ecology, Department of Life Sciences, University of Coimbra, 3000-456 Coimbra, Portugal
[2]Department of Life Sciences, University of Coimbra, Coimbra, Portugal
[3]Molecular Physical Chemistry R&D Unit, Department of Chemistry, University of Coimbra, Coimbra, Portugal
[4] Research Centre for Anthropology and Health, Department of Life Sciences, University of Coimbra, 3000-456 Coimbra, Portugal
[5]School of Technology of Tomar, Polytechnic Institute of Tomar, Tomar /Mação, Portugal.

*Corresponding author:
Mariana Pedrosa
Laboratory of Forensic Anthropology, Centre for Functional Ecology, Department of Life Sciences, University of Coimbra, 3000-456 Coimbra, Portugal
E-mail address: marianaslfpedrosa@gmail.com

Orcid:
Mariana Pedrosa – 0000-0001-9951-5765
Francisco Curate – 0000-0002-0480-209X
Luís A. E. Batista de Carvalho – 0000-0002-8059-8537
Maria Paula M. Marques – 0000-0002-8391-0055
Maria Teresa Ferreira – 0000-0002-2437-7780

Abstract
In Forensic Anthropology, the application of traditional methods for estimating the biological profile of human skeletal remains is often hampered by poor preservation and skeletal representativeness, compromising their reliability. Thus, the development of alternative methods to the morphometric analysis of bones to estimate the biological profile of human remains is paramount.
The age of an individual can cause changes in bone morphology, mass and size, as well as in its chemical composition. In this sense, the main objective of this research was to evaluate if the contents of bone collagen (Am/P), carbonate type A (API), carbonate type B (BPI), the relation between the carbonate content (types A and B) to type B carbonate (C/C), carbonate-phosphate ratio (C/P) and crystallinity index (CI), spectroscopic indices obtained from relationships between infrared absorption band intensities (FTIR-ATR), can be used as age-at-death predictors. A sample of femora and humeri from the 21st Century Identified Skeleton Collection (N=80, 44 females and 36 males) was employed.
Results show that, with advancing age, women's femora have lower CI values, but BPI and C/P indices increase, and that the deformation and disorder of the crystal lattice are probably affected by the integration of type B carbonate content of the femur.
The ratios analysed, especially the CI and the BPI, show potential to estimate age-at-death in human skeletal remains, when sex is already known, thus helping to assess the biological profile when conventional methods cannot be applied.

Keywords: Biological Profile; Bioapatite; IR Spectroscopy; Chemical Anthropology; Forensic Anthropology.

Introduction

The main goals of forensic anthropology include the identification of anonymous human remains. The assessment of the biological profile (*i.e.* ancestry, sex, age-at-death, and stature) comprises an essential step in the reconstructive identification procedure, with the identification of individualization factors, pathologies and/or anatomical variations, contributing to the positive identification of the individual, the exclusion of a suspect or the reduction in the number of missing people [1, 2]. The application of traditional anthropological methods for estimating the biological profile is often hampered by poor preservation and skeletal representativeness [1–3]. Other methods, such as DNA testing, involve costly and time-consuming destructive techniques [3,4]. Thus, the development of new methods for estimating the biological profile parameters from human skeletal remains is warranted in forensic contexts.

Bone is a heterogeneous material: of the total mass of bone, 60% is attributed to the inorganic phase (increasing to 70% in dry bone), 25% to the organic components, and about 10% to water [5, 6]. The organic fraction comprises proteins (mainly type I collagen) lipids, and a remaining 2% representing varied cellular constituents [7, 8]. The inorganic component, bioapatite, has a composition and structure similar to the apatite minerals, a low crystalline carbonated calcium phosphate mineral with the general formula $Ca_{10}(PO_4)_{6-x}(OH)_{2-y}(CO_3)_{x+y}$, being similar to hydroxyapatite when x=y=0 [9]. Although bone mineral is often referred to as hydroxyapatite in the literature, it is a misconception as it is a non-stoichiometric apatite and can be replaced by a wide variety of ions [9, 10]. The predominant substituent is carbonate ion (2 – 8% by weight), depending on the species, age and type of tissue (bone, enamel, dentin or pathological calcification), at two anionic sites of the hydroxyapatite structure: hydroxyl groups (type A) and phosphate (type B) in the hydroxyapatite matrix, the latter being the major type of substitution [10–14]. In addition, charge balancing is required [15]. Since carbonate groups (CO_3^{2-}) have a different phosphate charge and geometry (PO_4^{3-}) and are much larger than hydroxyl groups (OH^-), their presence in the crystal lattice generates distortions that lead to a decrease in the crystallinity of bioapatite [13, 16]. In addition to these substitutions, varying amounts of other ions such as fluorine (F^-), chloride (Cl^-), bromine (Br^-) and magnesium (Mg^{2+}) may also be incorporated into the crystal lattice depending on the chemical environment of the tissue [5, 17]. The relative quantities of bone tissue constituents, as well as their geometric and spatial arrangement, vary depending on several factors: age of the individual; age and type of tissue; diet; metabolism; pathological conditions; *post-mortem* interval; and body deposition conditions [18, 19].

Fourier Transform Infrared Spectroscopy (FTIR) is one of the most widely used techniques for analysing the structure and composition of bone material, since it is inexpensive and very effective and sensitive in the analysis of both bone mineral and organic components [9, 11, 14, 19–23]. The Attenuated Total Reflection (ATR) mode consists in a beam of radiation that enters a crystal with a high refractive index (usually zinc selenide (ZnSe) or diamond) and is reflected internally if the angle of incidence in the sample-crystal interface is greater than the critical angle [14, 24–27]. The interaction between radiation and the sample occurs on this surface and depends on the characteristics of the sample and the environment [14]. The advantage of FTIR-ATR not be a destructive technique is that intact bone samples can be analysed [24–27].

In recent years, infrared spectroscopy has become one of the most important tools for molecular characterization and identification and has been shown to be useful for biological anthropology [6, 9, 16,

20, 28, 29]. Nevertheless, research about changes in the chemical structure of bones in a forensic context are still scarce.

The inorganic fraction of the bone matrix has been extensively studied by infrared spectroscopy [9, 11, 14, 19–23]. The chemical structure of bone mineral is not static, containing a variety of inclusions and substitutions that evolve with age: both the carbonate content [29–33] and the crystallinity index (CI) increase [12, 32, 34, 35], but the amount of phosphate ions present in bioapatite is inversely proportional to age [32, 34, 36]. In a study of human osteons [12] and male baboons aged between birth and 32 years [37], the mean C/P ratio, also referred to as the ratio carbonate-mineral, increased with chronological age and crystallinity increased with age until it reached a plateau. However, Turunen et al. [38] stated that crystallinity is independent of the age of the animal. Moreover, Sillen and Morris [39] showed that all bones in the study had a relatively high crystallinity index, which was observed to increase irregularly with age. Age-related changes in crystallinity during growth and maturity are generally interpreted as an equilibrium resulting from the constant remodelling process [32]. Decreased protein production with age has been reported by Grynpas et al. [40]: trabecular bone in the human femoral neck of younger individuals (18-37 years) had more extracellular bone matrix proteins than those of individuals aged 51-79 years. This has also been demonstrated in undifferentiated osteoblast cultures obtained from human trabecular bone from embryo to 60 years old [41].

The aim of the present study was to evaluate whether spectroscopic indices (obtained through FTIR-ATR), namely bone collagen (Am/P); type A carbonate (API); type B carbonate (BPI), and the relationship between carbonate contents (A and B) and type B carbonate (C/C); and carbonate-phosphate ratio (C/P) and crystallinity index (CI), are associated with age and can be used as age-at-death predictors in human skeletal remains, particularly femora and humeri recovered from Santarém cemetery.

Materials and Methods

Sample

Eighty individuals from the 21st Century Identified Skeleton Collection (CEI/XXI) of the Laboratory of Forensic Anthropology of the University of Coimbra [42] were analysed. Individual ages-at-death ranged between 33 and 97 years old ($\bar{x}$ = 76.3; SD = 15.4), with the 43 females (55%) aged between 50 and 97 years ($\bar{x}$ = 82.0; SD = 10.9) and 37 males (45%) between 33 and 92 years ($\bar{x}$ = 69.3; SD = 17.2). Table 1 shows the distribution of the total sample by age groups and sex. The age-at-death distribution of the sample reflects the demographic profile of the CEI/XXI, a collection skewed towards older individuals.

The present study focused on two long bones from the same skeleton – the femur and the humerus – as they are more resistant to diagenetic effects [43]. The femora and humeri were mostly evaluated on the left side - except when they were subjected to surgical treatment (e.g., prosthesis), were burned or were exceedingly fragmented.

For chemical analysis, compact bone tissue was given preference in sample selection, as it is less susceptible to diagenesis [44]. All samples were collected from the long bones' midshaft (in the femur it was collected from the posterior portion and in the humerus from the anterior portion). The outer layer was removed by gentle sandpapering to prevent sample contamination. All samples were scraped, producing a powder suitable for FTIR-ATR, and stored in identified Eppendorf tubes.

Fourier-Transform Infrared Spectroscopy - Attenuated Total Reflection (FITR-ATR)

The FTIR-ATR spectra were acquired on a Bruker Optics Vertex 70 FTIR spectrometer purged by CO_2-free dry air in the mid-infrared range (400 - 4000 cm^{-1}) using a Platinum ATR single reflection diamond accessory, with a KBr beamsplitter and a liquid nitrogen cooled wide band Mercury Cadmium Telluride (MCT) detector in the QFM-UC laboratory. The spectra for each sample correspond to the sum of 128 scans, with a resolution of 2 cm^{-1} and apodized with a three-term Blackman-Harris function. The error in wavenumbers was estimated to be less than 1cm^{-1}. The spectra were corrected for the frequency dependence of the penetration depth of the electric field in ATR (considering a mean refection index of 1.25) using the Opus Spectroscopy Software, Version 7.2. The intensity of the bands was measured by absorbance through calculation of the maximum value (peak height) after baseline correction and spectra normalization (relative to the phosphate band, $\nu_3(PO_4^{3-})$, at about 1035 cm^{-1}). This resulted in a comparable baseline between spectra and different powder consistency [9]. To verify the spectral differences of bone samples, due to the variables under study, several mathematical relationships were applied, which are defined in Table 2.

Data Analysis

Subsequent statistical analysis of the spectroscopic data was performed with RStudio software that uses the R programming language for statistical computing and graphics [49]. A nonparametric test for independent variables, Mann-Whitney, was applied to evaluate the null hypothesis that the above indices are not different in the femur and the humerus. Relationships between the chemometric indices calculated for the femur and humerus and age-at-death (for the total sample and as a function of sex) were assessed using two correlation coefficients: Pearson and Spearman. For the test and each correlation coefficient performed, a significance level of 95% was adopted.

Whenever outliers were confirmed, they were not excluded from the database. Since the main objective of this work was to study how chemometrics vary with age-at-death, removing outliers would have been counterproductive and would bias the analyses.

Results

Differences between femur and humerus

Representative FTIR-ATR spectra (400–2000 cm^{-1}) from femur and humerus samples of the same individual are presented in Fig. 1. Signals corresponding to the main functional groups within the samples are observed: in the 450–650 cm^{-1} spectral region, bands corresponding to the out-of-plane bending vibrations of bioapatite´s phosphate; in the 900–1200 cm^{-1} interval, signals due to the stretching vibrational modes of PO_4^{3-}; in the 1450–1550 cm^{-1} range, bands assigned to the stretching modes of the carbonate ions (CO_3^{2-}), from its substitution by hydroxyl and phosphate groups in the biological apatite; lastly, bands assigned to the amide groups of bone´s protein constituents (mainly type I collagen), in the 1200–1800 cm^{-1} spectral region – amide I (1650 cm^{-1}), amide II (1500-1550 cm^{-1}) and amide III (1200-1300 cm^{-1}).

Descriptive statistics, including sample means and standard deviations, applied to the spectroscopic parameters measured for the bone samples are summarized in Table 3. In addition, the Mann-Whitney test

showed that there were statistically significant differences ($p < 0.05$) between the humerus and femur for all chemometric indices except API and protein content in females (Table 4), with femur and humerus type A carbonate content and Am/P values showing a similar distribution. Thus, for CI, the values are higher for the humerus, in females. In contrast, C/C has higher values for the male femurs, while both BPI and C/P are lower in male humeri.

Chemometric analysis and age-at-death

Overall, for the total sample, the CI, API and Am/P indices did not change significantly with age-at-death for both the femur and humerus samples (Tables 5 and 6). However, the femoral type B carbonate content is related to age-at-death (Pearson $p < 0.05$, $r = 0.2563$; Spearman $p < 0.05$, $\rho = 0.2397$), as well as the femoral carbonate to phosphate ratio (Pearson $p < 0.05$, $r = 0.2612$, Spearman $p < 0.05$, $\rho = 0.2434$) and the total carbonate (types A and B) to type B carbonate index (Pearson $p < 0.05$, $r = -0.2361$).

In the female samples, there was no statistically significant relationship between femoral and humeral API with age-at-death. However, the crystallinity index of the femur is significantly reduced with increasing age-at-death (Pearson $p < 0.01$, $r = -0.4337$; Spearman $p < 0.05$, $\rho = -0.3097$), as well as BPI (Pearson $p < 0.05$, $r = 0.3255$), C/P (Pearson $p < 0.05$, $r = 0.3492$; Spearman $p < 0.05$, $\rho = 0.3114$) and C/C (Pearson $p < 0.05$; $r = -0.3720$).

Regarding the male samples, there was no statistically significant association between age-at-death and any of the studied chemometric indices.

Discussion

Human bones are quite variable in structure, shape, and size, and these variables can somehow interfere with bone chemical parameters, especially with crystallinity [50]. The chemical composition of bone is very specific, regardless of bone type, although specificity varies with each index [9]. The noted dissimilarities between the femur and the humerus may be related to differences in bone structure and remodelling [51]. In addition, diagenetic changes and/or localized differences in the burial geochemical environment may motivate intra-individual variability [52].

The crystallinity index (CI) reflects a combination of the relative sizes of crystals and the extent to which atoms are ordered in the crystal lattice [53, 54]. CIs presently calculated are in accordance with the values obtained in previous studies [26, 28, 45, 46, 54, 55]. Unlike most studies reported in the literature [12, 31, 32, 34, 35, 56], the current results evidenced that not only there was no statistically significant relationship between CI and age-at-death in the overall sample [56], as it also decreased progressively with age-at-death in females. This suggests that with advancing age the crystal structure of bone becomes more disorganized and/or containing smaller crystals, leading to crystalline disorder [6, 57].

The smaller the size of the bone apatite nanocrystals, the larger the surface area compared to the same mass of larger size crystals. Physiologically, bioapatite crystals act as an ionic reservoir (*e.g.* Ca^{2+}). A larger surface area of the crystals results in a much larger percentage of constituent ions that can react with other ions and/or other organic constituents of extracellular fluids, rendering bioapatite relatively reactive [58, 59] and providing crystals with an ideal organization for exchanging these ions with extracellular (environmental) fluids.

According to Handschin and Stern [35], bone crystallinity increases substantially from birth until the age of 30. In turn, from the age of 30 to 80 the variation in bioapatite crystallinity seems negligible. These authors also noticed a slight decrease in crystallinity over the age of 80, which can be triggered by bone atrophy (osteoporosis) affecting the mature compact bone. In the present study, there were no individuals under 30 years of age, with only eight aged 30-60 years and 43 (>50% of the sample) with a chronological age-at-death of 80 years or older. In addition, in the female sample, 31 of the 44 women (71%) were very old (80 years of age or older) and none was under 30 years old, with no equitable distribution of age groups. The unbalanced age-at-death profile of the studied sample certainly influenced the comparative potential with previous works.

Besides the unequal age distribution, several factors may have contributed to the discrepancy between the CI values obtained in the present investigation and the results reported in the literature:

(i) the method applied to calculate the crystallinity index is distinct and/or not employing the same FTIR technique [60], as well as not performing ATR correction or carrying it out with a different average reflection index;

(ii) tissue heterogeneity. For example, according to Boskey et al. [56], in a sample of 22 patients (16 of them women), there is an increased crystallinity in the trabecular bone with age-at-death. However, Trueman and co-authors [47] state that there are no significant differences between cortical and trabecular bone crystallinity;

(iii) the duration of the swelling period may also affect the CI value in the most superficial layer of cortical bone, since crystallinity increases with the period of inhumation [47, 54]. Also, differences in the anatomical location of the sampling [9] or the statistical treatment of data (*e.g.*, clustering of decades *vs* linear regression) can lead to disparities in the results [47]. Likewise, studies in bones with very small sample sizes potentially provide fewer representative results, as measurement error can easily change the variability in the resulting CI [9, 61].

Previous studies have focused on faunal bones (e.g., [31, 34, 38, 62, 63]) and the available data in human skeletons is scarce. As faunal bones present differences in microstructure of mineralized tissues, differences in CI values can be found [9]. Moreover, there is a great diversity in bone proportion and composition between species, mainly due to inorganic groups (*e.g.*, phosphate and carbonate) [63–65]. Thus, the results obtained from faunal studies should not be extrapolated to experimental values acquired in human bone.

The carbonate to phosphate ratio indicates the level of carbonate substitution. According to Nielsen-Marsh and Hedges [66], fresh bone has C/P values of 0.34 ± 0.1. Although the results obtained from the carbonate-phosphate ratio are higher (0.370 ± 0.049), they are in agreement with other studies [9, 67], given that the analysed dry bones possibly gained carbonate from the burial environment [66].

The C/P index has a monotonic and directly proportional association with the age-at-death, as observed in several studies [36, 68, 69] having a greater expression in the female sample. However, according to Paschalis et al. [12], the CO_3^{2-}/PO_4^{3-} ratio reveals that it is inversely proportional to bone age. On the contrary, Rey and co-authors [31] describing the absolute carbonate content through the carbonate-phosphate ratio, reported that it increases with increasing bone age. Direct comparisons with these two studies should not be performed as bone age (biological age) and age-at-death (chronological age) are not

equivalent terms [70]. Moreover, there is a discrepancy between the results of the present investigation and those described by Paschalis et al. [12], since their study is limited to osteons. In addition, they used data obtained from only two patients.

In the present research it was found that there is a positive correlation between femoral BPI (CO_3^{2-} replacing PO_4^{3-} ions present in bioapatite) and age-at-death in the total sample, in females, in line with several published studies [12, 30, 31, 69].

The presence of type B CO_3^{2-} ions can be associated to the low mineral crystallinity in the cortical bone [30]. CO_3^{2-} replacement plays an important role in bone properties [31]. In addition, the amount of carbonate in biological apatite is known to affect the CI value, as the process of substitution of PO_4^{3-} by CO_3^{2-} produces smaller crystals (carbonate ions inhibit the growth of the bioapatite crystals) with higher structural stress (caused by distortions and defects in the crystal lattice). This may stem from the different charge and geometry of CO_3^{2-} relative to PO_4^{3-} ions, leading to an increased disorder and to a reduction of crystallographic perfection [55, 71, 72]. Additionally, samples with a high content of type B carbonates have a low CI value [46, 48, 53], which is consistent with the data obtained with the association of the two indices previously mentioned with age-at-death. Moreover, an increase in crystallinity can still produce a constant CI if carbonate compensation occurs [72]. Thus, a decreasing crystallinity and an increasing content of type B carbonates suggests that the carbonate ion can be a predominant factor in the biological regulation or control of crystallinity of biological apatite crystals.

The C/C index, in turn, represents the ratio of total (A+B) to type B carbonates. Their linear (weak) decrease with age-at-death demonstrates an increase of a disparate ratio of type A to type B carbonates, either caused by a decrease in the latter or an increase in the former. As mentioned above, it was found that, with increasing age, there is an increase in phosphate substitution by type B carbonates. However, no relationship was observed between age-at-death and type A carbonate, although Miller et al. [33] found an increase in type A carbonate content with bone crystal maturation. The values obtained for the C/C index may be explained by the influence of the band at 1460 cm^{-1}, $\delta(CH_2)_{collagen + lipid}$, given its partial overlap with the ν_3 $(CO_3^{2-})_{A+B}$ signal at 1450 cm^{-1} which may lead to misinterpretations [17, 62]. Therefore, the use of C/C in relation to age-at-death for forensic purposes should be followed with care.

Casuccio [73] found an increasing collagen content in the trabecular bone tissue of human lumbar vertebrae, while other authors reported a decrease in the amount of collagen in human femur and iliac bones with age [74, 75]. Similarly, Very and colleagues [76] observed a diminishing organic content with age-at-death (mainly through analysis of the collagen amide I band). Likewise, by analysing hydroxyproline, an essential amino acid present in collagen, Bailey and co-authors [77] concluded that the total collagen concentration in bone decreased with age, with no differences according to sex. The results obtained by Vassalo et al. [23] through the Am/P index (calculated as in the present study) support this hypothesis.

According to several researchers [78–80], collagen degradation begins early in life and gradually increases with age. Contrary to these studies, no effect of age on the collagen content (calculated using the Am/P formula described in Table 2) of either femur or humerus was found. This is in accordance with Dequeker and Merlevede [81] and Akkus et al. [57], who observed no association between collagen content and age for the iliac bone. One possible explanation for the discrepancies detected between different studies is the decrease in total bone mass with age, especially significant in women [82].

All correlations obtained with statistical significance in this study are modest, and extrapolation for future studies must be cautious, as larger sample sizes are needed, with a more equitable distribution of the age groups, in order to validate the observed trend.

Conclusions

The investigation of skeletal remains of unknown identity is a major goal in forensic anthropology, with age-at-death estimation being an important step for identification [2, 83].

FTIR-ATR is a highly sensitive and accurate spectroscopic tool for studying the physicochemical modifications of inorganic and organic fractions in bone tissue. The small amount of sample required for the analysis, its minimally invasive nature, low cost and easy quantification are major advantages when compared to other techniques. The development of a fast, direct and reliable technique to estimate the age-at-death from human skeletal remains, particularly for very incomplete or fragmented ones, is of the utmost relevance in forensic anthropology.

The application of the spectroscopic (infrared) indices Am/P, API, BPI, C/C, C/P and CI in human humeri and femora was performed with a view to show the potential relevance of chemometric analysis to age-at-death estimation, without resorting to osteometric and/or morphological analysis (which, in some instances, may not be possible).

With advancing age, especially in women, the crystalline structure of bone becomes more disordered, having larger deformations and smaller crystals due to a greater incorporation of type B carbonates in the crystal lattice, resulting in a decrease of the CI value and an increase in BPI and C/P. Some of these parameters (*e.g.* CI and BPI) have shown a promising potential for estimating age-at-death, especially for females. However, for an accurate understanding of the changes in these indices it is necessary to analyse a higher number of samples, from different bones and particularly from non-adults and young adults.

Acknowledgements

The authors thank the Centre for Functional Ecology, the Research Centre for Anthropology and Health and the Molecular Physical Chemistry R&D Unit (financed by national funds by FCT – Fundação para a Ciência e Tecnologia, under the projects UID/BIA/04004/2019, UID/SADG/00283/2019 and UIDB/00070/2020, respectively).

The authors state that they do not have any conflicts of interest to declare.

References

1. Cattaneo C (2007) Forensic anthropology: developments of a classical discipline in the new millennium. Forensic Sci Int 165:185–193. https://doi.org/10.1016/j.forsciint.2006.05.018
2. Cunha E (2014) A Antropologia Passo a Passo. In: Gomes A (ed) Enfermagem Forense. Lidel, Lisboa, pp 280–288
3. Mundorff AZ, Shaler R, Bieschke ET, Mar-Cash E (2014) Marrying Anthropology and DNA: Essential for Solving Complex Commingling Problems in Cases of Extreme Fragmentation. In: Adams BJ, Byrd JE (eds) Recovery, Analysis, and Identification of Commingled Human Remains. Academic Press, San Diego, pp 257–273
4. Yazedjian L, Kešetović R (2008) The Application of Traditional Anthropological Methods in a

DNA-Led Identification Process. In: Adams BJ, Byrd JE (eds) Recovery, Analysis, and Identification of Commingled Human Remains. Humana Press, pp 271–284
5. Boskey JA, Gokhale AL, Robey PG (2001) The Biochemistry of Bone. In: Marcus R, Feldman D, Nelson D, Rosen C (eds) Osteoporosis I. Academic Press, San Diego, pp 107–188
6. Wang X-Y, Zuo Y, Huang D, et al (2010) Comparative Study on Inorganic Composition and Crystallographic Properties of Cortical and Cancellous Bone. Biomed Environ Sci 23:473–480. https://doi.org/https://doi.org/10.1016/S0895-3988(11)60010-X
7. Boskey AL, Robey PG (2007) The Composition of Bone. In: Bilezikian JP, Bouillon R, Clemens T et al (eds) Primer on the Metabolic Bone Diseases and Disorders of Mineral Metabolism. Wiley-Blackwell, pp 84–92
8. Zhu W, Robey PG, Boskey AL (2013) The Regulatory Role of Matrix Proteins in Mineralization of Bone. In: Marcus R, Feldman D, Nelson D, Rosen C (eds) Osteoporosis I. Academic Press, San Diego, pp 235–255
9. Gonçalves D, Vassalo AR, Mamede AP, et al (2018) Crystal clear: Vibrational spectroscopy reveals intrabone, intraskeleton, and interskeleton variation in human bones. Am J Phys Anthropol 166:296–312. https://doi.org/10.1002/ajpa.23430
10. Nagy G, Lorand T, Patonai Z, et al (2008) Analysis of pathological and non-pathological human skeletal remains by FT-IR spectroscopy. Forensic Sci Int 175:55–60. https://doi.org/10.1016/j.forsciint.2007.05.008
11. Marques MPM, Gonçalves D, Amarante AIC, et al (2016) Osteometrics in burned human skeletal remains by neutron and optical vibrational spectroscopy. RSC Adv 6:68638–68641. https://doi.org/10.1039/c6ra13564a
12. Paschalis EP, DiCarlo E, Betts F, et al (1996) FTIR Microspectroscopic Analysis of Human Osteonal Bone. Calcif Tissue Int 59:480–487. https://doi.org/10.1007/BF00369214
13. Madupalli H, Pavan B, Tecklenburg MMJ (2017) Carbonate substitution in the mineral component of bone: Discriminating the structural changes, simultaneously imposed by carbonate in A and B sites of apatite. J Solid State Chem 255:27–35. https://doi.org/10.1016/j.jssc.2017.07.025
14. Mamede AP, Gonçalves D, Marques MPM, Batista de Carvalho LAE (2018) Burned bones tell their own stories: A review of methodological approaches to assess heat-induced diagenesis. Appl Spectrosc Rev 53:603–635. https://doi.org/10.1080/05704928.2017.1400442
15. Tacker RC (2008) Carbonate in igneous and metamorphic fluorapatite: Two type A and two type B substitutions. Am Mineral 93:168–176. https://doi.org/10.2138/am.2008.2551
16. Wopenka B, Pasteris JD (2005) A mineralogical perspective on the apatite in bone. Mater Sci Eng C 25:131–143. https://doi.org/10.1016/j.msec.2005.01.008
17. Carden A, Morris MD (2000) Application of vibrational spectroscopy to the study of mineralized tissues (review). J Biomed Opt 5:259. https://doi.org/10.1117/1.429994
18. Person A, Bocherens H, Saliège JF, et al (1995) Early Diagenetic Evolution of Bone Phosphate: An X-ray Diffractometry Analysis. J Archaeol Sci 22:211–221. https://doi.org/10.1006/jasc.1995.0023
19. Boskey A, Pleshko Camacho N (2007) FT-IR imaging of native and tissue-engineered bone and cartilage. Biomaterials 28:2465–2478. https://doi.org/10.1016/j.biomaterials.2006.11.043
20. Lebon M, Reiche I, Bahain JJ, et al (2010) New parameters for the characterization of diagenetic alterations and heat-induced changes of fossil bone mineral using Fourier transform infrared spectrometry. J Archaeol Sci 37:2265–2276. https://doi.org/10.1016/j.jas.2010.03.024
21. Marques MPM, Mamede AP, Vassalo AR, et al (2018) Heat-induced Bone Diagenesis Probed by Vibrational Spectroscopy. Sci Rep 8:15935. https://doi.org/10.1038/s41598-018-34376-w
22. Mamede AP, Vassalo AR, Piga G, et al (2018) Potential of Bioapatite Hydroxyls for Research on Archeological Burned Bone. Anal Chem 90:11556–11563. https://doi.org/10.1021/acs.analchem.8b02868
23. Vassalo AR, Cunha E, Batista de Carvalho LAE, Gonçalves D (2016) Rather yield than break:

assessing the influence of human bone collagen content on heat-induced warping through vibrational spectroscopy. Int J Legal Med 130:1647–1656. https://doi.org/10.1007/s00414-016-1400-x

24. Beasley MM, Bartelink EJ, Taylor L, Miller RM (2014) Comparison of transmission FTIR, ATR, and DRIFT spectra: implications for assessment of bone bioapatite diagenesis. J Archaeol Sci 46:16–22. https://doi.org/10.1016/j.jas.2014.03.008
25. Dutta A (2017) Fourier Transform Infrared Spectroscopy. In: Thomas S, Thomas R, Zachariah AK, Mishra RK (eds) Spectroscopic Methods for Nanomaterials Characterization. Elsevier Inc, pp 73–93
26. Thompson TJU, Gauthier M, Islam M (2009) The application of a new method of Fourier Transform Infrared Spectroscopy to the analysis of burned bone. J Archaeol Sci 36:910–914. https://doi.org/10.1016/j.jas.2008.11.013
27. Monnier GF (2018) A review of infrared spectroscopy in microarchaeology: Methods, applications, and recent trends. J Archaeol Sci Reports 18:806–823. https://doi.org/10.1016/j.jasrep.2017.12.029
28. Stiner MC, Kuhn SL, Surovell TA, et al (2001) Bone Preservation in Hayonim Cave (Israel): a Macroscopic and Mineralogical Study. J Archaeol Sci 28:643–659. https://doi.org/10.1006/jasc.2000.0634
29. Hollund HI, Ariese F, Fernandes R, et al (2013) Testing an alternative high-throughput tool for investigating bone diagenesis: FTIR in attenuated total reflection (ATR) mode. Archaeometry 55:507–532. https://doi.org/10.1111/j.1475-4754.2012.00695.x
30. Legros R, Balmain N, Bonel G (1987) Age-Related Changes in Mineral of Rat and Bovine Cortical Bone. Calcif Tissue Int 41:137–144. https://doi.org/10.1007/BF02563793
31. Rey C, Renugopalakrishman V, Collins B, Glimcher MJ (1991) Fourier Transform Infrared Spectroscopic Study of the Carbonate Ions in Bone Mineral During Aging. Calcif Tissue Int 49:251–258. https://doi.org/10.1007/BF02556214
32. Handschin RG, Stern WB (1995) X-Ray Diffraction Studies on the Lattice Perfection of Human Bone Apatite (Crista Iliaca). Bone 16: 355S–363S. https://doi.org/10.1016/S8756-3282(95)80385-8
33. Miller LM, Vairavamurthy V, Chance MR, et al (2001) In situ analysis of mineral content and crystallinity in bone using infrared micro-spectroscopy of the ν_4 PO_4^{3-} vibration. Biochim Biophys Acta - Gen Subj 1527:11–19. https://doi.org/10.1016/S0304-4165(01)00093-9
34. Grynpas MD, Bonar LC, Glimcher MJ (1984) Failure to Detect an Amorphous Calcium-Phosphate Solid Phase in Bone Mineral: A Radial Distribution Function Study. Calcif Tissue Int 36:291–301. https://doi.org/10.1007/BF02405333
35. Handschin RG, Stern WB (1992) Crystallographic Lattice Refinement of Human Bone. Calcif Tissue Int 51:111–120. https://doi.org/10.1007/BF00298498
36. Rey C, Kim HM, Glimcher MJ (1994) Maturation of Poorly Crystalline Synthetic and Biological Apatites. In: Brown PW, Constantz B (eds) Hydroxyapatite and Related Materials. CRC Press, Boca Raton, pp 181–187
37. Gourion-Arsiquaud S, Burket JC, Havill LM, et al (2009) Spatial Variation in Osteonal Bone Properties Relative to Tissue and Animal Age. J Bone Miner Res 24:1271–1281. https://doi.org/10.1359/jbmr.090201
38. Turunen MJ, Saarakkala S, Rieppo L, et al (2011) Comparison Between Infrared and Raman Spectroscopic Analysis of Maturing Rabbit Cortical Bone. Appl Spectrosc 65:595–603. https://doi.org/10.1366/10-06193
39. Sillen A, Morris A (1996) Diagenesis of bone from Border Cave: implications for the age of the Border Cave hominids. J Hum Evol 31:499–506. https://doi.org/10.1006/jhev.1996.0075
40. Grynpas MD, Tupy JH, Sodek J (1994) The Distribution of Soluble, Mineral-Bound, and Matrix-Bound Proteins in Osteoporotic and Normal Bones. Bone 15:505–513.

https://doi.org/10.1016/8756-3282(94)90274-7
41. Fedarko NS, Vetter UK, Weinstein S, Robey PG (1992) Age-Related Changes in Hyaluronan, Proteoglycan, Collagen, and Osteonectin Synthesis by Human Bone Cells. J Cell Physiol 151:215–227. https://doi.org/10.1002/jcp.1041510202
42. Ferreira MT, Vicente R, Navega D, et al (2014) A new forensic collection housed at the University of Coimbra, Portugal: The 21st century identified skeletal collection. Forensic Sci Int 245:202.e1-202.e5. https://doi.org/https://doi.org/10.1016/j.forsciint.2014.09.021
43. Boaks A, Siwek D, Mortazavi F (2014) The temporal degradation of bone collagen: A histochemical approach. Forensic Sci Int 240:104–110. https://doi.org/10.1016/j.forsciint.2014.04.008
44. Grupe G (1988) Impact of the Choice of Bone Samples on Trace Element Data in Excavated Human Skeletons. J Archaeol Sci 15:123–129. https://doi.org/10.1016/0305-4403(88)90002-7
45. Weiner S, Bar-Yosef O (1990) States of Preservation of Bones from Prehistoric Sites in the Near East: A survey. J Archaeol Sci 17:187–196. https://doi.org/10.1016/0305-4403(90)90058-D
46. Wright LE, Schwarcz HP (1996) Infrared and Isotopic Evidence for Diagenesis of Bone Apatite at Dos Pilas, Guatemala: Palaeodietary Implications. J Archaeol Sci 23:933–944. https://doi.org/10.1006/jasc.1996.0087
47. Trueman CNG, Behrensmeyer AK, Tuross N, Weiner S (2004) Mineralogical and compositional changes in bones exposed on soil surfaces in Amboseli National Park, Kenya: Diagenetic mechanisms and the role of sediment pore fluids. J Archaeol Sci 31:721–739. https://doi.org/10.1016/j.jas.2003.11.003
48. Snoeck C, Lee-Thorp JA, Schulting RJ (2014) From bone to ash: Compositional and structural changes in burned modern and archaeological bone. Palaeogeogr Palaeoclimatol Palaeoecol 416:55–68. https://doi.org/10.1016/j.palaeo.2014.08.002
49. Team RC (2019) R: A language and environment for statistical computing. http://r-project.org/. Accessed 4 November 2019
50. Reznikov N, Chase H, Brumfeld V, et al (2015) The 3D structure of the collagen fibril network in human trabecular bone: Relation to trabecular organization. Bone 71:189–195. https://doi.org/https://doi.org/10.1016/j.bone.2014.10.017
51. Thompson TJU, Islam M, Bonniere M (2013) A new statistical approach for determining the crystallinity of heat-altered bone mineral from FTIR spectra. J Archaeol Sci 40:416–422. https://doi.org/10.1016/j.jas.2012.07.008
52. Francalacci P, Tarli SB (1988) Multielementary Analysis of Trace Elements and Preliminary Results on Stable Isotopes in Two Italian Prehistoric Sites. Methodological aspects. In: Grupe G, Herrmann B (eds) Trace Elements in Environmental History. Proceedings in Life Sciences. Springer, Berlin, Heidelberg, pp 41–52
53. Shemesh A (1990) Crystallinity and diagenesis of sedimentary apatites. Geochim Cosmochim Acta 54:2433–2438. https://doi.org/https://doi.org/10.1016/0016-7037(90)90230-I
54. Stiner MC, Kuhn SL, Weiner S, Bar-Yosef O (1995) Differential Burning, Recrystallization, and Fragmentation of Archaeological Bone. J Archaeol Sci 22:223–237. https://doi.org/10.1006/jasc.1995.0024
55. Trueman CN, Privat K, Field J (2008) Why do crystallinity values fail to predict the extent of diagenetic alteration of bone mineral? Palaeogeogr Palaeoclimatol Palaeoecol 266:160–167. https://doi.org/10.1016/j.palaeo.2008.03.038
56. Boskey AL, DiCarlo E, Paschalis E, et al (2005) Comparison of mineral quality and quantity in iliac crest biopsies from high- and low-turnover osteoporosis: an FT-IR microspectroscopic investigation. Osteoporos Int 16:2031–2038. https://doi.org/10.1007/s00198-005-1992-3
57. Akkus O, Polyakova-Akkus A, Adar F, Schaffler MB (2003) Aging of Microstructural Compartments in Human Compact Bone. J Bone Miner Res 18:1012–1019. https://doi.org/10.1359/jbmr.2003.18.6.1012

58. Thompson TJU, Islam M, Piduru K, Marcel A (2011) An investigation into the internal and external variables acting on crystallinity index using Fourier Transform Infrared Spectroscopy on unaltered and burned bone. Palaeogeogr Palaeoclimatol Palaeoecol 299:168–174. https://doi.org/10.1016/j.palaeo.2010.10.044
59. Driessens FCM, van Dijk JWE, Borggreven JMPM (1978) Biological Calcium Phosphates and Their Role in the Physiology of Bone and Dental Tissues I. Composition and Solubility of Calcium Phosphates. Calcif Tissue Res 26:127–137. https://doi.org/10.1007/BF02013247
60. Glimcher MJ (2006) Bone: Nature of the Calcium Phosphate Crystals and Cellular, Structural, and Physical Chemical Mechanisms in Their Formation. Rev Mineral Geochemistry 64:223–282. https://doi.org/10.2138/rmg.2006.64.8
61. Surovell TA, Stiner MC (2001) Standardizing Infra-red Measures of Bone Mineral Crystallinity: an Experimental Approach. J Archaeol Sci 28:633–642. https://doi.org/10.1006/jasc.2000.0633
62. Rey C, Collins B, Goehl T, et al (1989) The Carbonate Environment in Bone Mineral: A Resolution-Enhanced Fourier Transform Infrared Spectroscopy Study. Calcif Tissue Int 45:157–164. https://doi.org/10.1007/BF02556059
63. Pleshko N, Boskey A, Mendelsohn R (1991) Novel Infrared spectroscopic method for the determination of crystallinity of hydroxyapatite minerals. Biophys J 60:786–793. https://doi.org/10.1016/S0006-3495(91)82113-0
64. Figueiredo MM, Gamelas JAF, Martins AG (2012) Characterization of Bone and Bone-Based Graft Materials Using FTIR Spectroscopy. In: Theophanides T (ed) Infrared Spectroscopy. IntechOpen, Rijeka, pp 315–338
65. Wang Q, Li W, Liu R, et al (2019) Human and non-human bone identification using FTIR spectroscopy. Int J Legal Med 133:269–276. https://doi.org/10.1007/s00414-018-1822-8
66. Nielsen-Marsh CM, Hedges REM (2000) Patterns of Diagenesis in Bone II: Effects of Acetic Acid Treatment and the Removal of Diagenetic CO_3^{2-}. J Archaeol Sci 27:1151–1159. https://doi.org/10.1006/jasc.1999.0538
67. Longato S, Wöss C, Hatzer-Grubwieser P, et al (2015) Post-mortem interval estimation of human skeletal remains by micro-computed tomography, mid-infrared microscopic imaging and energy dispersive X-ray mapping. Anal Methods 7:2917–2927. https://doi.org/10.1039/c4ay02943g
68. Akkus O, Adar F, Schaffler MB (2004) Age-related changes in physicochemical properties of mineral crystals are related to impaired mechanical function of cortical bone. Bone 34:443–453. https://doi.org/10.1016/j.bone.2003.11.003
69. Yerramshetty JS, Lind C, Akkus O (2006) The compositional and physicochemical homogeneity of male femoral cortex increases after the sixth decade. Bone 39:1236–1243. https://doi.org/10.1016/j.bone.2006.06.002
70. Klepinger LL (2006) Fundamentals of Forensic Anthropology. John Wiley & Sons, New Jersey
71. Rey C, Combes C, Drouet C, et al (2007) Physico-chemical properties of nanocrystalline apatites: Implications for biominerals and biomaterials. Mater Sci Eng C 27:198–205. https://doi.org/10.1016/j.msec.2006.05.015
72. Pucéat E, Reynard B, Lécuyer C (2004) Can crystallinity be used to determine the degree of chemical alteration of biogenic apatites? Chem Geol 205:83–97. https://doi.org/10.1016/j.chemgeo.2003.12.014
73. Casuccio C (1962) An Introduction to the Study of Osteoporosis (Biochemical and Biophysical Research in Bone Ageing). Proc R Soc Med 55:663–668. https://doi.org/10.1177/003591576205500815
74. Rogers HJ, Weidmann SM, Parkinson A (1952) Studies on the skeletal tissues. II. The collagen content of bones from rabbits, oxen and humans. Biochem J 50:537–542. https://doi.org/10.1042/bj0500537
75. Eastoe JE (1968) Chemical aspects of the matrix concept in calcified tissue organisation. Calcif Tissue Res 2:1–19. https://doi.org/10.1007/BF02279189

76. Very JM, Gibert R, Guilhot B, et al (1997) Effect of Aging on the Amide Group of Bone Matrix, Measured by FTIR Spectrophotometry, in Adult Subjects Deceased as a Result of Violent Death. Calcif Tissue Int 60:271–275. https://doi.org/10.1007/s002239900228
77. Bailey AJ, Sims TJ, Ebbesen EN, et al (1999) Age-Related Changes in the Biochemical Properties of Human Cancellous Bone Collagen: Relationship to Bone Strength. Calcif Tissue Int 65:203–210. https://doi.org/10.1007/s002239900683
78. Zioupos P, Currey JD, Hamer AJ (1999) The role of collagen in the declining mechanical properties of aging human cortical bone. J Biomed Mater Res 45:108–116. https://doi.org/10.1002/(SICI)1097-4636(199905)45:2<108::AID-JBM5>3.0.CO;2-A
79. Collins MJ, Nielsen-Marsh CM, Hiller J, et al (2002) The survival of organic matter in bone: A review. Archaeometry 44:383–394. https://doi.org/10.1111/1475-4754.t01-1-00071
80. Ruppel ME, Burr DB, Miller LM (2006) Chemical makeup of microdamaged bone differs from undamaged bone. Bone 39:318–324. https://doi.org/10.1016/J.BONE.2006.02.052
81. Dequeker J, Merlevede W (1971) Collagen content and collagen extractability pattern of adult human trabecular bone according to age, sex and amount of bone mass. Biochim Biophys Acta - Gen Subj 244:410–420. https://doi.org/10.1016/0304-4165(71)90243-1
82. Dequeker J, Remans J, Franssen R, Waes J (1971) Ageing patterns of trabecular and cortical bone and their relationship. Calcif Tissue Res 7:23–30. https://doi.org/10.1007/BF02062590
83. Baccino E, Schmitt A (2006) Determination of Adult Age at Death in the Forensic Context. In: Schmitt A, Cunha E, Pinheiro J (eds) Forensic Anthropology and Medicine: Complementary Sciences From Recovery to Cause of Death. Humana Press, Totowa, NJ, pp 259–280

Average FTIR–ATR spectra, in the mid-infrared region, for femora and humeri samples from the 21st Century Identified Skeletal Collection

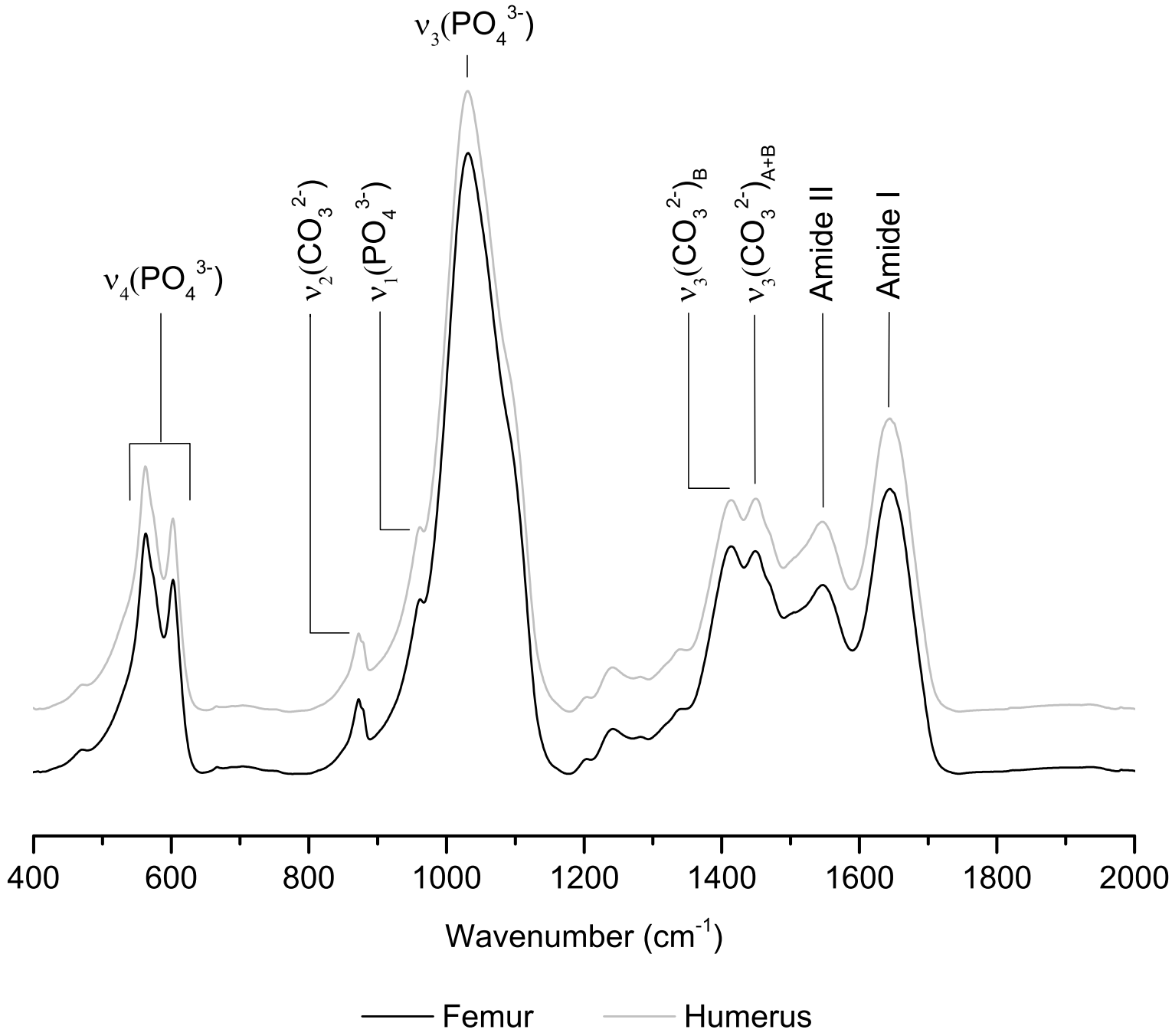

Table 1 Distribution of the total sample by age groups and sex (CEI/XXI)

Table 1 Distribution of the total sample by age groups and sex (CEI/XXI)

Age Group	Total		Male		Female	
	n	%	*n*	%	*n*	%
30-39	4	5.0	4	11.1	0	0
40-49	2	2.5	2	5.6	0	0
50-59	2	2.5	1	2.8	1	2.3
60-69	13	16.2	7	19.4	6	13.6
70-79	16	20.0	11	30.5	5	11.4
80-89	31	38.8	9	25.0	22	50.0
90+	12	15.0	2	5.6	10	22.7
Total	80	100	36	100	44	100

Table 2 Quantitative relationships used to evaluate the chemical composition of bone samples and publications relevant to protocol details (adapted from [14])

Parameter	Spectral relationship	Reference
Cristallinity Index (CI)	$\frac{\text{Abs}(602\ \text{cm}^{-1}) + \text{Abs}(562\ \text{cm}^{-1})}{\text{Abs}(590\ \text{cm}^{-1})}$	[45]
Carbonate to Phosphate (C/P)	$\frac{\text{Abs}(1415\ \text{cm}^{-1})}{\text{Abs}(1035\ \text{cm}^{-1})}$	[26, 46, 47]
Type A Carbonate (API)	$\frac{\text{Abs}(1540\ \text{cm}^{-1})}{\text{Abs}(603\ \text{cm}^{-1})}$	[48]
Type B Carbonate (BPI)	$\frac{\text{Abs}(1415\ \text{cm}^{-1})}{\text{Abs}(603\ \text{cm}^{-1})}$	[48]
Carbonate (A+B) to Carbonate B (C/C)	$\frac{\text{Abs}(1450\ \text{cm}^{-1})}{\text{Abs}(1415\ \text{cm}^{-1})}$	[26, 48]
Bone Collagen Content (Am/P)	$\frac{\text{Abs}(1650\ \text{cm}^{-1})}{\text{Abs}(1035\ \text{cm}^{-1})}$	[26]

Table 3 Descriptive statistics of parameters calculated from FTIR-ATR data

		n	CI		API		BPI		C/C		C/P		Am/P	
			$\bar{x}$	σ	$\bar{x}$	σ	$\bar{x}$	σ	$\bar{x}$	σ	$\bar{x}$	σ	$\bar{x}$	σ
Femur	Female	44	3.176	0.122	1.003	0.112	1.205	0.145	0.983	0.028	0.376	0.046	0.469	0.041
	Male	36	3.184	0.183	0.931	0.078	1.154	0.164	0.984	0.042	0.361	0.052	0.442	0.029
	Total	80	3.179	0.151	0.971	0.104	1.182	0.155	0.983	0.035	0.370	0.049	0.456	0.039
Humerus	Female	44	3.299	0.191	0.999	0.119	1.125	0.193	1.013	0.046	0.350	0.062	0.475	0.045
	Male	36	3.295	0.189	0.968	0.094	1.091	0.149	1.015	0.043	0.339	0.050	0.464	0.043
	Total	80	3.297	0.189	0.985	0.109	1.110	0.174	1.014	0.044	0.345	0.057	0.470	0.044

$\bar{x}$: mean; σ: standard deviation

Table 4 Descriptive statistics and Mann-Whitney test results on the differences in the median (M_d) of the chemical indexes calculated for the total sample, men and women

Index	Sex	Bone	M_d	ci95%	MW	*p-value*
CI	Female	Femur	3.141	3.139 – 3.213	620	< 0.01
		Humerus	3.334	3.241 – 3.357		
	Male	Femur	3.115	3.122 – 3.246	410	< 0.001
		Humerus	3.328	3.231 – 3.359		
	Total	Femur	3.134	3.146 – 3.213	2021	< 0.001
		Humerus	3.331	3.255 – 3.339		
API	Female	Femur	0.993	0.969 – 1.037	1031	**0.342**
		Humerus	0.976	0.963 – 1.035		
	Male	Femur	0.917	0.905 – 0.957	482	**0.604**
		Humerus	0.964	0.936 – 0.999		
	Total	Femur	0.958	0.948 – 0.994	2921	**0.062**
		Humerus	0.975	0.961 – 1.009		
BPI	Female	Femur	1.200	1.161 – 1.249	1213	< 0.05
		Humerus	1.086	1.066 – 1.184		
	Male	Femur	1.197	1.099 – 1.209	832	< 0.05
		Humerus	1.101	1.040 – 1.141		
	Total	Femur	1.197	1.148 – 1.217	4035	< 0.01
		Humerus	1.094	1.071 – 1.148		
C/C	Female	Femur	0.973	0.974 – 0.991	611	< 0.01
		Humerus	1.018	0.999 – 1.027		
	Male	Femur	0.966	0.969 – 0.998	355	<0.001
		Humerus	1.019	1.000 – 1.029		
	Total	Femur	0.972	0.975 – 0.991	1896	< 0.001
		Humerus	1.018	1.004 – 1.023		
C/P	Female	Femur	0.373	0.362 – 0.390	1220	< 0.05
		Humerus	0.344	0.331 – 0.369		
	Male	Femur	0.374	0.344 – 0.379	842	< 0.05
		Humerus	0.345	0.322 – 0.356		
	Total	Femur	0.373	0.358 – 0.380	4080	< 0.01
		Humerus	0.344	0.332 – 0.358		
Am/P	Female	Femur	0.472	0.456 – 0.481	867	**0.404**
		Humerus	0.477	0.461 – 0.488		
	Male	Femur	0.443	0.432 – 0.451	464	< 0.05
		Humerus	0.456	0.449 – 0.478		
	Total	Femur	0.454	0.448 – 0.465	2598	< 0.05
		Humerus	0.472	0.460 – 0.479		

ci95%: 95% confidence level; MW: value of the Mann-Whitney test

Table 5 Results of Pearson correlation coefficients (r) between CI, API, BPI, C/C, C/P and Am/P chemometric indices and age-at-death for the total sample and according to sex

Table 5 Results of Pearson correlation coefficients (*r*) between CI, API, BPI, C/C, C/P and Am/P chemometric indices and age-at-death for the total sample and according to sex

		Total			**Female**			**Male**		
		n	*r*	*p-value*	*n*	*r*	*p-value*	*n*	*r*	*p-value*
Femur	CI	80	-0.121	0.285	**44**	**-0.4337**	**0.0033****	36	0.0422	0.8069
	API	80	0.1557	0.1679	44	0.0202	0.8964	36	0.0100	0.9536
	BPI	**80**	**0.2563**	**0.0217***	**44**	**0.3213**	**0.0335***	36	0.1366	0.4271
	C/C	**80**	**-0.2361**	**0.0350***	**44**	**-0.3720**	**0.0130***	36	-0.1901	0.2668
	C/P	**80**	**0.2612**	**0.0193***	**44**	**0.3492**	**0.0201***	36	0.1364	0.4276
	Am/P	80	0.1246	0.2708	44	0.0278	0.8579	36	-0.0845	0.6243
Humerus	CI	80	-0.0186	0.8700	44	-0.1716	0.2655	36	0.0885	0.6078
	API	80	0.0066	0.9539	44	-0.2149	0.1612	36	0.0899	0.6023
	BPI	80	0.0820	0.4698	44	0.0230	0.8820	36	0.0732	0.6715
	C/C	80	-0.1117	0.3238	44	-0.1535	0.3199	36	-0.0864	0.6164
	C/P	80	0.1071	0.3444	44	0.0753	0.6270	36	0.0767	0.6568
	Am/P	80	-0.0338	0.7658	44	-0.2234	0.1449	36	0.0063	0.9711

* significant for $\alpha = 0.05$ ** significant for $\alpha = 0.01$

Table 6 Table 6 Results of Spearman correlation coefficients (ρ) between CI, API, BPI, C/C, C/P and Am/P chemometric indices and age-at-death for the total sample and according to

Table 6 Results of Spearman correlation coefficients (ρ) between CI, API, BPI, C/C, C/P and Am/P chemometric indices and age-at-death for the total sample and according to sex

		Total			**Female**			**Male**		
		n	ρ	*p-value*	*n*	ρ	*p-value*	*n*	ρ	*p-value*
Femur	CI	80	-0.1047	0.3555	**44**	**-0.3097**	**0.0408***	36	0.0624	0.7179
	API	80	0.0890	0.4323	44	-0.0027	0.9862	36	-0.0734	0.6704
	BPI	**80**	**0.2397**	**0.0322***	44	0.2908	0.0555	36	0.1358	0.4297
	C/C	80	-0.1047	0.3552	44	-0.1029	0.5063	36	-0.1908	0.2650
	C/P	**80**	**0.2434**	**0.0296***	**44**	**0.3114**	**0.0397***	36	0.1211	0.4817
	Am/P	80	0.0682	0.5476	44	-0.0044	0.9775	36	-0.1989	0.2448
Humerus	CI	80	-0.0764	0.5004	44	-0.1000	0.5184	36	0.0327	0.8497
	API	80	-0.0933	0.4103	44	-0.2845	0.0613	36	0.0478	0.7819
	BPI	80	0.0599	0.5975	44	-0.0392	0.8007	36	0.0778	0.6519
	C/C	80	-0.1111	0.3264	44	-0.1080	0.4851	36	-0.0352	0.8386
	C/P	80	0.0798	0.4814	44	-0.0042	0.9786	36	0.0682	0.6929
	Am/P	80	-0.1123	0.3214	44	-0.2420	0.1135	36	-0.0725	0.6742

* significant for $\alpha = 0.05$